

# Deep Learning Techniques for In-Crop Weed Identification: A Review

Kun Hu<sup>a,\*</sup>, Zhiyong Wang<sup>a</sup>, Guy Coleman<sup>b</sup>, Asher Bender<sup>c</sup>, Tingting Yao<sup>d</sup>,  
Shan Zeng<sup>e</sup>, Dezhen Song<sup>f</sup>, Arnold Schumann<sup>g</sup>, Michael Walsh<sup>b</sup>

<sup>a</sup>*School of Computer Science, The University of Sydney, NSW 2006, Australia*

<sup>b</sup>*School of Life and Environmental Sciences, The University of Sydney,  
NSW 2006, Australia*

<sup>c</sup>*Australian Centre for Field Robotics, The University of Sydney, NSW 2008, Australia*

<sup>d</sup>*College of Information Science and Technology, Dalian Maritime University,  
Dalian 116000, China*

<sup>e</sup>*College of Mathematics and Computer Science, Wuhan Polytechnic University,  
Hubei 430023, China*

<sup>f</sup>*Department of Computer Science and Engineering, Texas A&M University,  
College Station, TX 77843-3127, USA*

<sup>g</sup>*Citrus Research and Education Center, University of Florida, Florida 33850-2299, USA*

---

## Abstract

Weeds are a significant threat to the agricultural productivity and the environment. The increasing demand for sustainable agriculture has driven innovations in accurate weed control technologies aimed at reducing the reliance on herbicides. With the great success of deep learning in various vision tasks, many promising image-based weed detection algorithms have been developed. This paper reviews recent developments of deep learning techniques in the field of image-based weed detection. The review begins with an introduction to the fundamentals of deep learning related to weed detection. Next, recent progresses on deep weed detection are reviewed with the discussion of the research materials including public weed datasets. Finally, the challenges of developing practically deployable weed detection methods are summarized, together with the discussions of the opportunities for future research. We hope that this review will provide a timely survey of the field and attract more researchers to address this inter-disciplinary research problem.

---

\*Corresponding author

Email address: hukun\_sdu@hotmail.com (Kun Hu)

*Keywords:* Weed management, precision agriculture, deep learning

---

## 1. Introduction

Due to their competition with crops for water, nutrients and sunlight, weeds are a significant threat to agricultural productivity [1, 2]. Weed control in conservation cropping systems is reliant on the use of herbicides due to the lack of suitable alternative weed control options that do not interfere with the minimum tillage, residue retention principles, and thus benefits of these systems. To alleviate this threat, precise weed management becomes an increasingly important approach that is implemented through site-specific weed control (SSWC) techniques to identify and target weeds with treatments such as herbicides, lasers, electrical weeding and targeted tillage [3].

While in-crop SSWC creates important opportunities for improved production, the major challenge for these systems is the development of robust weed identification algorithms that perform accurately and consistently in complex and highly variable crop production environments [4]. The majority of previous methods have been based on conventional computer vision and machine learning techniques in both colour and multispectral imagery (e.g., [5]). These approaches often follow a pipeline in which hand-crafted image features play a primary role. As a result, developing such pipelines is labour intensive and images are required to be captured within well-defined conditions.

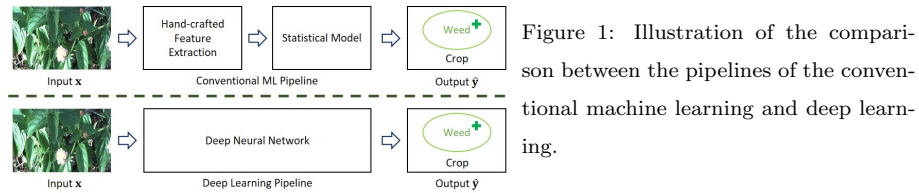


Figure 1: Illustration of the comparison between the pipelines of the conventional machine learning and deep learning.

Fortunately, due to the great success of deep learning in many vision tasks, hand-crafted features are no longer required to derive promising results. Instead, deep representations of an input image can be obtained using deep learning, which are relevant to the task at hand. For weed identification, four types

of deep learning approaches are illustrated in Fig. 2: a) image classification identifies the weed or the crop species contained in an image; b) object detection identifies the per-weed locations of the plants within an image; c) semantic segmentation conducts pixel-wise classification of individual weed classes and d) instance segmentation further identifies the instance of each pixel belonging to. As most of the deep learning-based weed identification studies are based on existing and well-known deep architectures, the architectures relevant to weed identification, including their building blocks and contributions, are introduced first. Next more than 30 deep learning-based weed identification studies are discussed in terms of their architectures, goals and performance. In addition, as deep learning based weed identification research often requires a large volume of annotated data, we provide the details of current publicly available weed datasets and benchmarking metrics.

Expanding on the research of existing well-known architectures, we present other fine-grained and alternative architectures that may offer advantages in terms of the identification performance for future research. For practice purposes, there are still limitations and challenges of current research to provide weed control in large-scale crop production systems. Therefore, deep learning mechanisms which could further improve the efficiency and effectiveness of weed control including real-time inference, weakly-supervised learning, explainable learning and incremental learning techniques are discussed.

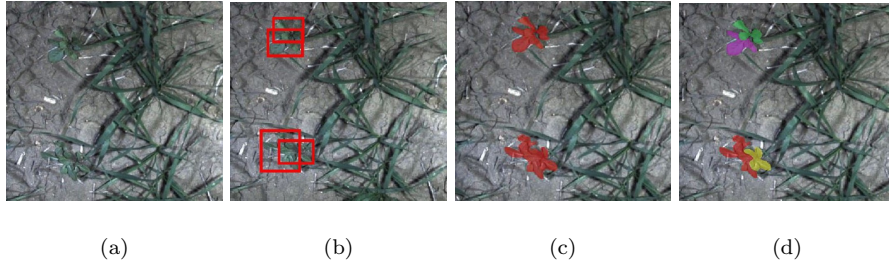


Figure 2: Illustration of the four major approaches for weed detection: (a) image classification (b) object detection (c) semantic segmentation (d) instance segmentation.

In summary, this review aims to: 1) investigate deep learning techniques

related to weed control; 2) summarize current deep learning-based weed identification research including architectures, research materials and evaluation methods; 3) identify further challenges and improvements for future research with deep learning-based solutions.

The remainder of the review is organized as follows. In Section 2, deep learning architectures related to weed control are introduced. Section 3 provides a discussion of the existing deep learning based weed detection studies. In addition, public datasets and evaluation metrics for benchmarking are summarised. Section 4 discusses the challenges for weed detection and potential deep learning solutions. Finally, Section 5 concludes this review.

## 2. Overview of Deep Learning Techniques

In this section, the theory of deep learning techniques is introduced including the deep learning building blocks and architectures relevant for weed detection.

### 2.1. Machine Learning

Machine learning (ML) algorithms are a class of algorithms that 'learn' to perform a specific task given sample data (i.e., training data). These algorithms are not explicitly programmed with rules or instructions to fulfil the task. In general, a set of samples for a ML task  $\mathbf{D} = \{(\mathbf{x}_i, \mathbf{y}_i)\}$  can be obtained, where  $\mathbf{x}_i \in \mathbf{R}^p$  is the observed features describing the characteristics of the  $i$ -th sample and  $\mathbf{y}_i$  is the associated output. In general, for  $(\mathbf{x}, \mathbf{y}) \in \mathbf{D}$ , it can be costly and time-consuming to obtain  $\mathbf{y}$ , whilst  $\mathbf{x}$  is convenient to collect. Therefore, it is expected to learn a model  $f_{\Theta}(\mathbf{x})$  that maps input values to the target variable  $\hat{\mathbf{y}}$  as close as possible, where  $\Theta$  is a set containing parameters of the model. Optimization methods can be used to find the best set of model parameters,  $\hat{\Theta}$ , to minimize the difference between the predicted output  $\hat{\mathbf{y}} = f_{\hat{\Theta}}(\mathbf{x})$  and the ground truth  $\mathbf{y}$ . In regard to the form of  $\mathbf{y}$ , machine learning problems can be differentiated as classification problems if the value of  $\mathbf{y}$  is categorical, or regression problems if the value of  $\mathbf{y}$  is continuous.

In the past decades, various machine learning models have been proposed (e.g. support vector machines [6]). However, these methods require carefully devised hand-crafted features. Thanks to the recent growth in computational capacity and the availability of a large amount of training data, deep learning automatically integrates feature extraction and modelling together, and gains promising performance for many tasks. Fig. 1 provides an illustration of the difference between conventional machine learning vs. deep learning. In the following subsections, the details of deep learning are introduced.

## 2.2. Neural Networks

The model  $f_{\Theta}$  in machine learning can be chosen as a neural network (NN) [7], which contains an interconnected group of nodes (i.e., artificial neurons) inspired and simplified by the biological neural networks in animal brains. The most well-known neural network architectures are the multi-layered perceptrons (MLPs), shown in Fig. 3 (a). This architecture organizes nodes into groups of layers and connects nodes between neighbouring layers. In detail, the computations of the  $k$ -th layer can be written as:

$$\mathbf{x}^{(k)} = \sigma(\mathbf{W}^{(k)}\mathbf{x}^{(k-1)} + \mathbf{b}^{(k)}), \quad (1)$$

where  $\mathbf{x}^{(k)} \in \mathbf{R}^{p^{(k)}}$  is the input of the  $k$ -th layer which can be viewed as  $p^{(k)}$  nodes of the neural network;  $\mathbf{W}^{(k)} \in \mathbf{R}^{p^{(k)} \times p^{(k-1)}}$  with the bias vector  $\mathbf{b}^{(k)} \in \mathbf{R}^{p^{(k)}}$  represents a linear transform of the input signal which introduces full connectivity between the  $(k-1)$ -th layer and the  $k$ -th layer;  $\sigma$  is an activation function which introduces a non-linearity to the output, allowing complex representations. In particular,  $\mathbf{x}^{(0)}$  is the input feature of a sample in  $D$ .

The layer defined in Eq. (1) can also be referred to as a fully connected (FC) layer. By stacking multiple FC layers, neural networks are able to formulate more complex representations of the input. To obtain predictions, computations are conducted from the first (input) layer to the last (output) layer, which is known as a forward propagation stage. To optimize the parameters  $\Theta = \{\mathbf{W}^{(k)}, \mathbf{b}^{(k)}\}$  of a neural network, a backward propagation stage updates the

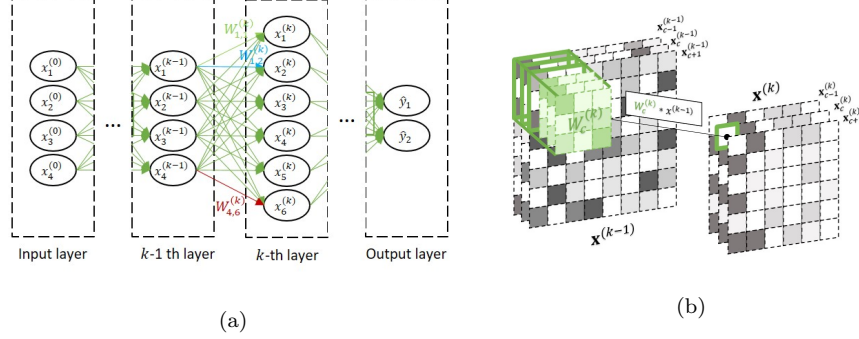


Figure 3: (a) Illustration of MLPs with input layer, hidden layers, and output layer. (b) Illustration of the convolution filter  $\mathbf{W}_c^{(k)}$  that operates with the input  $\mathbf{x}^{(k-1)}$  and outputs the  $c$ -th channel of  $\mathbf{x}^{(k)}$ .

parameters in an inverse order. Recently, more mechanisms and architectures have been proposed for constructing deeper neural networks, of which the ones related to weed identification are reviewed in the rest of this section.

### 2.3. Convolution Neural Networks

Inspired by the biological processes of animal visual cortex, convolution neural networks (CNNs) reduce the challenges of training deep models for visual tasks [8]. Convolution layers are the key components of CNNs, as illustrated in Fig. 3 (b). It involve partial connections compared with fully connected layers of MLPs, where each node focuses on a local region of the input. In detail, denote  $W^{(k)} = \{W_1^{(k)}, W_2^{(k)}, \dots, W_{C^{(k)}}^{(k)}\}$  to represent a series of  $C^{(k)}$  convolution filters and the computations of the  $k$ -th convolution layer can be written as:

$$\mathbf{x}_c^{(k)} = \sigma(\mathbf{W}_c^{(k)} * \mathbf{x}^{(k-1)} + \mathbf{b}^{(k)}), \quad (2)$$

where  $*$  represents a convolution operator and  $\sigma$  is an activation function;  $\mathbf{x}^{(k-1)}$  is the input feature map containing  $C^{(k-1)}$  channels and the output feature map is  $\mathbf{x}^{(k)} = (\mathbf{x}_1^{(k)}, \dots, \mathbf{x}_{C^{(k)}}^{(k)})$  containing  $C^{(k)}$  channels. A convolution layer can be viewed as a special case of FC layers with a sparse weight matrix.

Convolution layers often reduce the input spatial size but increase the number of channels. For some applications, recovery from a deep representation to

the original input size is required. For this purpose, deconvolution (transpose convolution) operations were used. Readers can refer to [9] for more details.

#### 2.4. Graph Neural Networks

Whereas most neural networks were designed for processing vectorized data, there are a wide range of applications involving non-vectorized data. Graph neural networks (GNNs) were devised for graph inputs. One commonly used GNN is graph convolution neural networks (GCNNs), which is a generalisation of the conventional CNNs by involving adjacency patterns [10]. In detail, a particular form to compute graph convolutions in  $k$ -th layer can be written as:

$$\mathbf{X}^{(k)} = \sigma(\mathbf{X}^{(k-1)} \mathbf{A} \mathbf{W}^{(k)} + \mathbf{b}^{(k)}), \quad (3)$$

where  $\mathbf{X}^{(k)} \in \mathbf{R}^{n \times p^{(k)}}$  represents the vertex features of  $n$  vertices in a graph,  $\mathbf{A} \in \mathbf{R}^{n \times n}$  is an adjacency matrix to illustrate the relations between vertices,  $\mathbf{W}^{(k)} \in \mathbf{R}^{p^{(k-1)} \times p^{(k)}}$  contains trainable weights and  $\mathbf{b}^{(k)}$  is a bias vector. Instead of using pre-defined adjacency matrix, graph attention network (GAT) estimated edge weights of the adjacency in line with the vertex features [11]. Recently, various methods were proposed to focus on some graph characteristics, which could not be captured by GCNNs (e.g. longest circle in [12]).

#### 2.5. Deep Learning Architectures

Following the above discussed neural networks for deep learning, various deep learning architectures can be constructed in line with different target applications. In terms of weed detection tasks, four categories of deep neural network architectures are summarized, including image classification, object detection, semantic segmentation, and instance segmentation.

##### 2.5.1. Image Classification

Image classification tasks focus on predicting the category (e.g. weed species) of the object in an input image. Input images can be viewed as spatially organized data, and many CNN based architectures have been proposed for classi-

fying them into a specific class or category. AlexNet, which consists of 5 convolution layers and 3 fully connected layers was first adopted for large scale image classification [13]. Convolution layers (potentially with other mechanisms) were used to formulate deep representations from input images and FC layers were further used to generate output vectors in line with the categories involved. VGG [14] further introduced convolution filters with a  $3 \times 3$  perception field to substitute each convolution filter with a large perception field to learn a deeper representation and reduce the computational costs. InceptionNet was further proposed to introduce filters of multiple sizes at the same level to characterize the salient regions in an image, which can have extremely large variations in size [15]. With the growing depth of the CNN architectures, short-cuts between the layers alleviate the gradient vanishing issues [16], such as ResNet and DenseNet. NASNet [17] was obtained by architecture search algorithms.

### *2.5.2. Object Detection*

Object detection aims to identify the positions and the classes of the objects contained in an image. Generally, various CNN architectures for image classification can be used as backbones to learn deep representations and specific output layers can be introduced to obtain object-level annotations including positions and categories. For example, R-CNN and its improvements such as Faster R-CNN [18] were proposed with a two-stage scheme where the first stage generates regional proposals and the second stage predicts the positions and labels for those proposals. One-stage methods were also explored to perform object detection with less latency. For example, YOLO [19] (You Only Look Once) was proposed by treating object detection as a regression problem, of which the output is a feature map containing the positions and labels of each pre-defined grid cell. Single shot multi-box detector (SSD) [20] introduced feature maps of multiple scales and prior anchor boxes of different ratios. As class imbalance is one of the critical challenges for one-stage object detection, RetinaNet with focal loss was proposed [21]. Note that pre-defined anchor boxes played an important role for most of the above mentioned methods. To avoid



the significant computational costs to compute such anchor boxes, anchor-free methods were also investigated in [22].

### 2.5.3. *Semantic Segmentation*

Semantic segmentation focuses on the pixel-wise (dense) predictions of an image, by which the category of each pixel is identified. In general, semantic segmentation uses fully convolution networks (FCNs), which were first explored in [23]. These studies often involved an encoder-decoder scheme: the encoder formulates a latent representation of an image through convolutions and the decoder focuses on upsampling of the latent representation to the original image size for dense predictions. By increasing the capacity of the decoder, U-Net [24] was proposed with promising performance for medical images. SegNet [25] additionally involved pooling indices for its decoder, compared with the general encoder-decoder models to use the pooled values only, to perform non-linear upsampling to keep the boundary information. Pyramid scene parsing network (PSPNet) and different-region-based context aggregation by a pyramid pooling module [26] exploited the capability of global context as a superior framework for pixel-level predictions. Instead of following a conventional encoder-decoder scheme, DeepLab models adopted atrous convolutions to reduce the downsampling operations with a large reception field [27].

### 2.5.4. *Instance Segmentation*

Instance segmentation aims to output both the class and class instance information for individual pixels. Instance segmentation methods were initially devised in a two-stage manner by focusing on two separated tasks: object detection and semantic segmentation. For example, Mask R-CNN [28] was proposed using a top-down design, which first conducts object detection task to locate the bounding boxes of each instance and next within each bounding box undertakes semantic segmentation. Bottom-up methods were also investigated, which first conduct semantic segmentation and use clustering or metric learning to obtain different instances (e.g. [29]). Two-stage methods require accurate results

from each stage and the computation cost of two-stage methods could be expensive. Therefore, single shot methods were explored. Anchor-based methods YOLACT [30] introduced two parallelized tasks to an existing one-stage object detection model including a dictionary of non-local prototype masks over the entire image and predicting a set of linear combination coefficients per instance. An anchor-free method fully convolutional instance-aware semantic segmentation (FCIS) was proposed based on FCNs by introducing position-sensitive inside/outside score maps [31]. PolarMask [32] conducted instance center classification and dense distance regression in a polar coordinate, which is a much simpler and flexible framework. Very recently, BlendMask [33] inspired by FCIS introduced a blender module to effectively combine instance-level information and semantic information with low-level fine-granularity.

### 3. Deep Learning for Weed Identification

In this section, deep learning based weed identification studies are summarized covering four approaches: image classification, object detection, semantic segmentation and instance segmentation. Before reviewing those approaches, research data, data augmentation and evaluation metrics used in these studies are reviewed first to provide a context in the field.

#### 3.1. Weed Data

Weed data is the foundation for developing and benchmarking weed identification methods, and sensing technologies will determine what weed data can be acquired and what weed management practice can be developed [34]. While various sensing techniques like ultrasound, LiDAR (Light Detection And Ranging) and optoelectronic sensors were used for simple differentiation between weeds and crops, image-based weed identification has gained increasing interests due to the advances of various imaging techniques.

Multispectral imaging captures light energy within specific wavelength ranges or bands of the electromagnetic spectrum, which can capture information beyond visible wavelength [35]. For example, hyperspectral images consist of many

contiguous and narrow bands; near infrared (NIR) imaging uses a subset of the infrared band, as the pigment in plant leaves, chlorophyll, strongly absorbs red and blue visible light and reflects near infrared. Driven by the low cost RGB cameras and the significant progresses in computer vision, RGB images have been increasingly used (e.g. [4]). In addition, some studies involved depth images (the distance between the image plane and each pixel) [36, 37].

The availability of rich public datasets in the field plays a key role in facilitating the development of new algorithms specific to weed identification tasks. In recent years, a number of in-crop weed datasets have been made public, as shown in Fig. 4, and will be reviewed in the rest of this section.

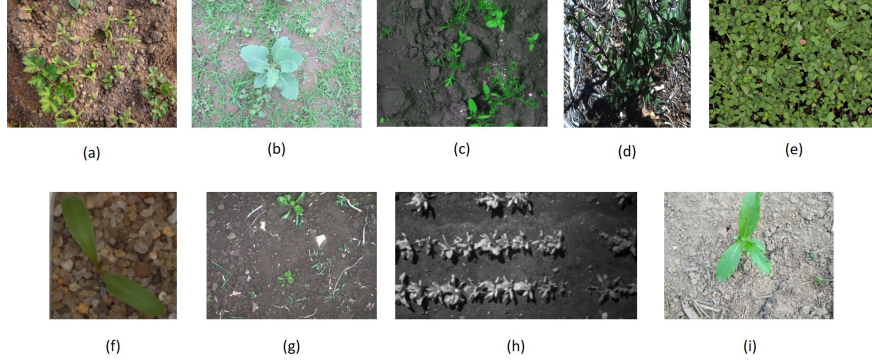


Figure 4: Sample weed images from several public datasets. (a) Carrot-Weed [38] (b) CWF-788 [39] (c) CWF-ID [40] (d) DeepWeeds [4] (e) GrassClover [41] (f) Plant Seedlings Dataset [42] (g) Sugar Beets 2016 [43] (h) Sugar Beet/Weed Dataset [44] (i) Weed-Corn/Lettuce/Radish [45].

**Bccr-segset** [46] contains 30,000 RGB images with pixel-wise annotations collected of canola (*Brassica napus*), maize (*Zea mays*) and wild radish (*Raphanus raphanistrum*). The images were acquired using an gantry-system mounted above an indoor growth facility across multiple growth stages.

**Carrot-Weed** [38] contains 39 RGB images collected with a 10-MP (Mega Pixel) phone camera under variable light conditions of young carrot (*Daucus carota subsp. sativus*) seedlings in the Republic of Macedonia. Pixel-level annotations were provided of three categories: carrots, unspecified weeds and soil

(<https://github.com/lameski/rgbweedddetection>).

**Crop/Weed Field Image Dataset** (CWFID) [40] comprises 60 top-down field images of carrots with intra-row and close-to-crop weeds captured by RGB cameras. Pixel-level annotations are provided for crop vs weed discrimination of 162 carrot plants and 332 weeds in total (<https://github.com/cwfid>).

**CWF-788** [39] is a field image dataset containing 788 RGB images collected from cauliflower (*Brassica oleracea var. botrytis*) fields with high weed pressure. It was collected for semantic segmentation of the cauliflower plants from the background (combining both weeds and soil) with manually segmented annotations (<https://github.com/ZhangXG001/Real-Time-Crop-Recognition>).

**DeepWeeds** [4] was collected from remote rangelands in northern Australia for weed specific image classification. It includes 17,509 images of 8 types of target weed species with various off-target plants native to Australia. The target weed species include chinee apple (*Ziziphus mauritiana*), lantana (*Lantana camara*), parkinsonia (*Parkinsonia aculeata*), parthenium (*Parthenium hysterophorus*), prickly acacia (*Vachellia nilotica*), rubber vine (*Cryptostegia grandiflora*), siam weed (*Chromolaena odorata*) and snake weed (*Stachytarpheta* spp.). For each target weed species (positive class), around 1,000 images were obtained; off-target flora and backgrounds not containing the weeds of interest are collected as a single negative class of 9,106 images. It was collected from 8 different locations with an attempt to balance scene bias images of the target species, and negative cases were collected at each location in similar quantities (<https://github.com/AlexOlsen/DeepWeeds>).

**Grass-Broadleaf** [47] contains 22 different plant species at early growth stages, which was constructed by combining 6 image datasets. In total, 10,413 RGB images were included. Note that image background was removed in this dataset and each image only contains one individual plant.

**GrassClover** [41] is a diverse image and biomass dataset, of which 8,000 synthetic RGB images are provided with pixel-wise annotations for semantic segmentation based weed identification studies. The dataset was collected in an outdoor field setting including 6 classes: unspecified grass species, white

clover (*Trifolium repens*), red clover (*Trifolium pratense*), shepherd’s purse (*Capsella bursa-pastoris*), unspecified thistle, dandelion (*Taraxacum* spp.) and soil. In addition, 31,600 unlabelled images were provided for pre-training, weakly-supervised learning, and unsupervised learning (<https://vision.eng.au.dk/grass-clover-dataset>).

**Plant Seedling Dataset** [42] contains 960 unique plants at several growth stages in RGB images for species including blackgrass (*Alopecurus myosuroides*), charlock (*Sinapis arvensis*), cleavers (*Galium aparine*), common chickweed (*Stellaria media*), wheat, fat hen (*Chenopodium album*), loose silky-bent (*Apera spica-venti*), maize (*Zea mays*), scentless mayweed, shepherd’s purse, small-flowered cranesbill (*Geranium pusillum*) and sugar beet (*Beta vulgaris* var. *altissima*) (<https://vision.eng.au.dk/plant-seedlings-dataset>).

**Soybean/Grass/Broadleaf/Soil** [48] comprises 15,336 segments of soybean (*Glycine max*), unspecified grass weeds, unspecified broadleaf weeds and soil. The segments were extracted using the simple linear iterative clustering (SLIC) superpixel algorithm on 400 images collected with an Unmanned Aerial Vehicle (UAV)-mounted RGB camera.

**Sugar Beets 2016** [43] was collected from agricultural fields with pixel-wise annotations for three classes: sugar beet, weeds, and soil. This dataset contains 1,600 images, of which 700 images were captured at first and 900 images were captured after a four-week period. Both RGB-D and multispectral images were provided, which is helpful to explore the effectiveness of different modalities for weed identification and to construct multi-modal learning methods (<http://www.ipb.uni-bonn.de/data/sugarbeets2016>).

**Sugar Beet/Weed Dataset** [44] contains 155 multispectral images (near-infrared 790 nm, red 660 nm) plus normalised difference vegetation index (NDVI) with pixel-wise labelling for sugar beet, weeds and soil from a controlled field experiment (<https://github.com/inkyusa/weedNet>).

**Weed-Corn/Lettuce/Radish** [45] contains 7,200 RGB images with image-level annotations. It includes three subsets: the maize dataset (1,200 images) was collected from a corn field with four different weed species (4,800

images) including Canada thistle (*Cirsium arvense*), fat hen, bluegrass (*Poa* spp.) and sedge (*Carex* spp.); the lettuce dataset was collected from a vegetable field of two plant classes including lettuce (500 images) and weeds (300 images); the radish dataset contains 200 radish images and 200 weeds images [38] (<https://github.com/zhangchuanyin/weed-datasets>).

Whilst these datasets provide useful imagery and annotation data for benchmarking, there is a lack of consistency and details in metadata reporting standards and contextual information. An understanding of weed species, beyond a simple awareness of the difference to crops, is important in creating opportunities to deliver specific weed control treatments. For example, contextual understanding of crop growth stages, presence/absence of stubble will assist in developing algorithms capable of handling variability across different conditions.

### 3.2. Data Augmentation

Due to the laborious nature of developing annotated datasets within weed control contexts, existing datasets are often not large enough and do not reflect sufficient diversity in conditions. A significant risk for deep learning using small datasets is overfitting, where the model performs well on the training set but performs poorly when being deployed in the fields. To address this issue, various data augmentation strategies were adopted to enlarge the size and the quality of the training sets such as random cropping, rotation, flipping, color space transformation, noise injection, image mixing, random erasing and generative approaches. Readers can refer to [49] for more details.

### 3.3. Evaluation Metrics

A number of metrics have been utilized to evaluate the performance of weed identification algorithms. The definition of these metrics may differ in terms of different types of identification approaches.

For binary image classification whereby the classification result of an input sample is labelled either as a positive (P) or a negative (N) case, 4 possible outcomes can be derived: (1) If a positive sample is classified as positive, the

prediction is correct and defined as **true positive** (TP). (2) If a negative sample is classified as positive, the prediction is **false positive** (FP). (3) If a negative sample is classified as negative, the prediction is **true negative** (TN). (4) If a positive sample is classified as negative, the prediction is **false negative** (FN).

Based on these definitions, some widely used evaluation metrics can be defined for benchmarking the performance of different algorithms. **Accuracy** measures the proportion of the correct predictions ( $\#TP + \#TN$ ) over all the predictions ( $\#P + \#N$ ). **Sensitivity**, also known as **recall**, measures the proportion of the correctly predicted positive cases ( $\#TP$ ) over all the positive cases ( $\#TP + \#FN$ ). It indicates the likelihood that the algorithm identifies all weeds. A low sensitivity would suggest that a large number of weeds are missed, while a sensitivity rate 1 indicates that all weeds are successfully detected. **Precision** measures the proportion of the correctly predicted positive cases ( $\#TP$ ) over all predicted positive cases ( $\#TP + \#FP$ ). For weed detection, a high precision indicates low off-target or crop damage. **Specificity** measures the proportion of the correctly predicted negative cases ( $\#TN$ ) over all predicted negative cases ( $\#TN + \#FP$ ). A low specificity suggests that an algorithm is delivering an control option towards crops. **F-score** (also known as **F<sub>1</sub> score**) combines the precision and the recall values by treating them with equal importance:

$$F_1 = 2 \cdot \frac{Precision \cdot Recall}{Precision + Recall}. \quad (4)$$

As a binary classification model generally outputs continuous predictions, a threshold is required to judge the predicted labels: if the score is beyond the threshold, the corresponding sample is predicted as a positive case; otherwise the sample is predicted as a negative case. By varying the threshold, trade-offs among some metrics can be made. A receiver operating characteristic curve (**ROC curve**) illustrates the diagnostic ability of a binary classification model by plotting the sensitivity against the 1-specificity at various threshold settings. A precision-recall curve (**PR curve**) shows plots the precision against the recall. A large area under these curves (**AUC**) often indicates a model of high quality. For multi-class classification, most of the these metrics can be computed class

by class and the mean of these metrics can be used.

For an object detection task with only one class, a sample is associated with an object in a bounding box. For a predicted bounding box, **intersection over union** (IoU) is defined as the area of the intersection divided by the area of the union of the predicted bounding box and a ground truth bounding box. Given a threshold  $\theta$ , if the confidence value of a predicted bounding box is beyond  $\theta$  and the IoU against the ground truth bounding box is beyond 0.5, the predicted bounding box is regarded as a TP case; if the confidence is beyond  $\theta$  and the IoU is less than 0.5, it is regarded as a FP case; if the confidence is less than  $\theta$  and the IoU is less than 0.5, it is regarded as a TN case; if the confidence is less than  $\theta$  and the IoU is beyond 0.5, it is regarded as a FN case. Next, the precision and recall values can be defined to measure the quality of detection results. By varying  $\theta$ , a PR curve can be obtained and **average precision** (AP):  $\int_0^1 p(r)dr$  is used to summarize the quality of the PR curve, where  $p(r)$  indicates the precision value  $p$  corresponding to the recall values  $r$  for a particular IoU threshold. In practice, different estimations for AP are adopted such as the AUC of the PR curve. Different IoU threshold values other than 0.5 can also be used to select the bounding boxes from the candidates and the corresponding AP can be obtained. For example,  $AP_{50}$  and  $AP_{75}$  define the AP with IoU threshold 0.5 and 0.75, respectively. For multi-class object detection problems, these metrics can be computed for each class individually and a **mean average precision** (mAP) can be obtained over all classes.

In segmentation tasks, a sample can be viewed as a pixel. The metrics such as (mean) accuracy (mAcc), recall, precision and F-score discussed above can be derived in a similar manner. By organizing the pixels belonging to the same class as regions, the concepts such as mAP and mIoU can be derived as well.

### 3.4. Weed Identification Methods

Existing studies on weed identification can be organized into four categories in terms of the approaches they used: weed image classification, weed object detection, weed object segmentation or weed instance segmentation. Tables 1,



Table 1: Summary of image classification based weed identification studies.

| Architecture                           | Type        | Dataset                         | Public Avail. | Target Species                  | AUC  | Acc. | Prec. | Recall Sens. | $F_1$ Score | Spec. |
|--|-------------|---------------------------------|---------------|---------------------------------|------|------|-------|--------------|-------------|-------|
| <b>Hyperspectral (400 - 1000nm)</b>    |             |                                 |               |                                 |      |      |       |              |             |       |
| Customized CNN (500X500) [35]          | Multiclass  |                                 | Y             | 4 weeds                         | -    | 94.7 | -     | -            | -           | -     |
| Customized CNN (250X250) [35]          | Multiclass  | UNSW Hyperspectral              | Y             | 4 weeds                         | -    | 90.6 | -     | -            | -           | -     |
| Customized CNN (125X125) [35]          | Multiclass  | Weed Dataset                    | Y             | 4 weeds                         | -    | 86.3 | -     | -            | -           | -     |
| FCNN-SPLBP (100X100) [50]              | Multiclass  |                                 | Y             | 4 weeds                         | -    | 89.7 | -     | -            | -           | -     |
| <b>Multispectral (NIR &amp; RGB)</b>   |             |                                 |               |                                 |      |      |       |              |             |       |
| FCNN-SPLBP [50]                        | Multiclass  | Sugar beet/weed Dataset         | Y             | crops, weeds, mix               | -    | 96.4 | -     | -            | -           | -     |
| <b>RGB</b>                             |             |                                 |               |                                 |      |      |       |              |             |       |
| ResNet-18 [51]                         | Binary      | Bean                            | -             | bean, weeds                     | 94.8 | -    | -     | -            | -           | -     |
| ResNet-18 [51]                         | Binary      | Spinach                         | -             | spinach, weeds                  | 95.7 | -    | -     | -            | -           | -     |
| AgroAVNET [52]                         | Multiclass  | Plant Seedling Dataset          | Y             | 3 crops, 9 weeds                | -    | 93.6 | 93.0  | 94.0         | 93.0        | -     |
| GCN-ResNet-101 [45]                    | Binary      | Radish                          | Y             | radish, weeds                   | -    | 98.9 | 98.5  | 98.3         | 98.9        | 98.5  |
| GCN-ResNet-101 [45]                    | Binary      | Corn                            | Y             | corn, weeds                     | -    | 97.8 | 99.3  | 99.2         | 99.3        | 97.1  |
| GCN-ResNet-101 [45]                    | Binary      | Lettuce                         | Y             | lettuce, weeds                  | -    | 99.4 | 98.4  | 99.7         | 99.0        | 99.0  |
| GCN-ResNet-101 [45]                    | Binary      | Mixed Dataset                   | Y             | 3 crops, weeds                  | -    | 96.5 | 98.8  | 98.7         | 97.2        | 96.5  |
| ResNet-50 [4]                          | Multiclass* |                                 | Y             | 8 weeds, others                 | -    | 95.7 | 95.7  | -            | -           | 98.0  |
| DenseNet-128-32 [53]                   | Multiclass* |                                 | Y             | 8 weeds, others                 | -    | 90.1 | -     | -            | -           | -     |
| GraphWeedsNet [54]                     | Multiclass* | DeepWeeds                       | Y             | 8 weeds, others                 | -    | 98.1 | 98.2  | -            | -           | 99.3  |
| DeepCluster VGG-16 [47]                | Multiclass  |                                 | Y             | 8 weeds, others                 | -    | 70.6 | 96.6  | -            | -           | -     |
| Customized Residual Net (128X128) [47] | Multiclass  | Combination of 6 Public Dataset | Y             | 22 (crops + weeds)              | -    | 86.2 | -     | -            | -           | -     |
| Customized Residual Net (128X128) [47] | Multiclass  | Grass-Broadleaf                 | Y             | soil, soybean, grass, broadleaf | -    | 89.1 | 66.3  | -            | -           | -     |
| AlexNet [48]                           | Multiclass  |                                 | Y             | soil, soybean, grass, broadleaf | -    | 99.5 | -     | 99.5         | -           | -     |
| K-means pre-training and CNN [55]      | Multiclass  | in-house                        | -             | soybean, 3 weeds                | -    | 92.9 | -     | -            | -           | -     |
| VGGNet [56]                            | Multiclass  | in-house                        | -             | 3 weeds                         | -    | -    | 98.2  | 99.1         | 98.6        | -     |
| VGGNet [56]                            | Multiclass  | in-house                        | -             | 3 weeds                         | -    | -    | 98.6  | 93.4         | 95.6        | -     |
| VGGNet [57]                            | Multiclass  | in-house                        | -             | 3 weeds                         | -    | -    | 95.1  | 99.1         | 97.1        | -     |
| VGGNet [57]                            | Multiclass  | in-house                        | -             | 3 weeds                         | -    | -    | 93.7  | 99.9         | 96.7        | -     |
| PCANet [58]                            | Multiclass  | in-house                        | -             | 91 weed seeds                   | -    | 91.0 | -     | -            | -           | -     |

\* Multi-label classification problem.

Table 2: Summary of object detection based weed identification studies.

| Architecture               | Target Species               | Modality | Prec. | Recall | $F_1$ Score | mIoU |
|----------------------------|------------------------------|----------|-------|--------|-------------|------|
| Faster R-CNN [59]          | 5 weeds                      | RGB      | 66.0  | 68.0   | 67.0        | 0.84 |
| DetectNet (1224X1024) [60] | weeds                        | RGB      | 86.6  | 46.3   | 60.3        | 0.64 |
| YOLOv4 [61]                | broadleaves, sedges, grasses | RGB      | 100.0 | 91.0   | 95.0        | -    |
| DetectNet (1280X720) [57]  | <i>Poa annua</i>             | RGB      | 100.0 | 99.6   | 99.8        | -    |
| DetectNet (1280X720) [57]  | <i>Poa annua</i>             | RGB      | 100.0 | 99.8   | 100.0       | -    |

Table 3: Summary of semantic segmentation based weed identification studies.

| Architecture                                | Dataset         | Target Species                                    | Public Avail. | $F_1$ Score | Prec. | Recall | mIoU | mAcc | mAP  | AUC  |
|---|-----------------|---|---------------|-------------|-------|--------|------|------|------|------|
| <b>Multispectral (NIR &amp; RGB), Depth</b> |                 |   |               |             |       |        |      |      |      |      |
| Customized U-Net [36]                       | Sugarbeets2016  | sugar beet, weeds, soil                           | Y             | 83.4        | -     | -      | -    | -    | -    | -    |
| DeepLabv3+ [37]                             | Sugarbeets2016  | sugar beet, weeds, soil                           | Y             | -           | -     | -      | 87.1 | -    | -    | -    |
| <b>Multispectral (NIR &amp; RGB)</b>        |                 |   |               |             |       |        |      |      |      |      |
| Customized CNNs (sNet + cNet) [62]          | in-house        | crops, weeds, soil                                | -             | -           | -     | -      | -    | 92.0 | 97.4 | -    |
| Customized FCN [63]                         | BONN            | crops, weeds, soil                                | Y             | 86.6        | 93.3  | 81.5   | -    | -    | -    | -    |
| Customized FCN [63]                         | STUTTGART       | crops, weeds, soil                                | -             | 92.4        | 91.6  | 93.5   | -    | -    | -    | -    |
| SegNet [44]                                 | Sugar beet/Weed | crops, weeds, soil                                | Y             | 80.0        | -     | -      | -    | -    | -    | 78.0 |
| VGG-UNet [64]*                              | Sugar beet/Weed | crops, weeds, soil                                | Y             | -           | -     | -      | -    | 95.0 | -    | -    |
| <b>RGB</b>                                  |                 |   |               |             |       |        |      |      |      |      |
| Customized CNN [65]                         | in-house        | carrots, weeds, soil                              | -             | 98.6        | 98.5  | -      | -    | 97.9 | -    | -    |
| U-Net + VGG-16 [66]                         | Sunflower       | sunflower, weed, soil                             | -             | -           | -     | -      | 80.0 | -    | -    | -    |
| AgNet [67]                                  | CWFID           | carrots, weeds, soil                              | Y             | -           | -     | -      | -    | 88.9 | -    | -    |
| MiniInception [67]                          | CWFID           | carrots, weeds, soil                              | Y             | -           | -     | -      | -    | 89.9 | -    | -    |
| Customized VGG-16 [68]                      | in-house        | maize, weeds, soil                                | -             | -           | -     | -      | 84.0 | 96.4 | -    | -    |
| Customized CNN with ResNet-10 Backbone [39] | CWF-788         | cauliflower, weeds, soil                          | Y             | 98.0        | -     | -      | 95.9 | -    | -    | -    |
| DeepLabv3+ [37]                             | Oilseed Image   | oilseed, weeds, soil                              | -             | -           | -     | -      | 88.9 | -    | -    | -    |
| VGG16-D [69]                                | in-house        | equipment,soil,stump, weeds,grass,radish, unknown | -             | -           | -     | -      | 55.0 | 79.0 | -    | -    |
| FCN-8s [41]                                 | GrassClover     | grass, white clover, red clover, weeds, soil      | Y             | -           | -     | -      | -    | -    | -    | -    |
| SegNet [38]                                 | Carrot-Weed     | carrots, weeds, soil                              | Y             | -           | -     | -      | -    | 64.1 | -    | -    |
| SegNet (ResNet-50 Backbone) [70]            | in-house        | canola, weeds                                     | -             | 99.3        | -     | -      | 82.9 | 99.5 | -    | -    |

\* additional information involved from NVDI modality.

2, 3 summarize the major studies of the first three categories, whilst instance segmentation based weed identification has emerged recently.

#### 3.4.1. Weed Image Classification

This approach aims to achieve image-level weed identification, determining of what species an image contains. An early deep learning based study [47] devised a residual CNN for multi-class classification. On their proposed Grass-Broadleaf dataset which contains 10,413 RGB crop-weed images of 22 weed species, an accuracy 86.2% was achieved. A variant PCA (Principal Component Analysis) network was proposed for classifying 91 classes of weed seeds using RGB images, and an accuracy 90.96% was achieved. AlexNet was adopted to classify RGB images from the public dataset - Grass-Broadleaf [48], which achieved an accuracy 99.5%. Although these results look promising, the plants or seeds were well segmented and the field or natural background information was limited, which could lead to failures under real field conditions.

More recently, a hybrid model of AlexNet and VGGNet was proposed. It was evaluated on a public plant seedling dataset containing RGB images of 3 crop species and 9 weed species at an early growth stage and achieved an accuracy 93.6%. Classifying three weed species including *Euphorbia maculata*, *Glechoma hederacea* and *Taraxacum officinale* growing in perennial ryegrass was studied [56] using VGGNet on RGB images. It achieved F-scores 98.6% and 95.6% for two independent test sets collected from two fields with different locations. A similar study was also conducted to classify three other species of weeds growing in perennial ryegrass including *Hydrocotyle spp*, *Hedyotis corymbosa* and *Richardia scabra* [57]. Another study identified cephalanoplos, digitaria, bindweed and soybean in RGB images by introducing a CNN based on LeNet-5 [71] with a K-means clustering for unsupervised pre-training, which achieved an accuracy 92.9% [55]. To further advance weed image classification in complex environments, a public dataset, namely DeepWeeds [4], was constructed by acquiring RGB images in remote and extensive rangelands with rough and uneven terrains. The baseline accuracy 95.7% was achieved by a ResNet-50 for

multi-label classification. A simplified DenseNet, namely DenseNet-128-32, was explored to reduce the computational cost and inference time, while keeping the performance comparable to that of the original DenseNet model [53].

Recently, a few fine-grained architectures were explored to improve weed image classification performance. By introducing graph-based image representation, a graph weeds net achieved the state-of-the-art accuracy 98.1% on the DeepWeeds dataset, which formulated global and fine-grained weed characteristics with GCNs [54]. Another study also investigated the graph mechanisms [45], in which GCN-ResNet-101 was proposed and the accuracy values varied from 96.5% to 98.9% on 4 public RGB datasets.

Deep unsupervised learning was explored in a recent weed study [72], which explored two methods: joint unsupervised learning of deep representations and image clusters (JULE) and deep clustering for unsupervised learning of visual features (DeepCluster). They adopted the CNN outputs as features for a clustering algorithm and specified pseudo labels for samples based on the clustering results. As reported, the DeepCluster method achieved an accuracy 70.6% with a VGG-16 backbone on the DeepWeeds dataset, and an accuracy 99.5% with an AlexNet backbone on Grass-Broadleaf.

Besides RGB images, multispectral imaging has also been investigated. Different sizes of multispectral images with a CNN involving 4 convolution layers were explored [35]. By varying the input size from  $125 \times 125$  to  $500 \times 500$ , the accuracy varied from 86.3% to 94.7% on the UNSW Hyperspectral Weed Dataset. FCNN-SPLBP combined CNN and superpixel based local binary pattern feature extraction [50], which was evaluated on two public datasets: an accuracy 89.7% for  $100 \times 100$  pixel images on the UNSW Hyperspectral Weed Dataset and an accuracy 96.4% on the sugar beet/weed dataset.

### 3.4.2. Weed Object Detection

Existing weed object detection methods are mainly based on generic object detection methods. In [60], DetectNet was used with an mIoU 64.0 and an F-score 60.3 on an in-house dataset containing 1,427 RGB images. Another

study [57] with DetectNet achieved F-scores 99.8% and 100.0% for two different environments in detecting a weed species, namely *Poa annua*. In [59], Faster R-CNN achieved an mIoU 84.0% and an F-score 67.0% in detecting water-hemp (*Amaranthus tuberculatus*), Palmer amaranthus (*Amaranthus palmeri*), common lambsquarters (*Chenopodium album*), velvetleaf (*Abutilon theophrasti*), and foxtail species such as yellow and green foxtails on an in-house dataset containing 450 augmented RGB images. YOLOv3 was used to detect broadleaves, sedges and grasses [61] and achieved an F-score 95.0%.

### 3.4.3. Weed Semantic Segmentation

An intuitive approach for weed semantic segmentation is based on a two-stage scheme. Two CNNs were devised in [62], namely sNet and cNet, in which the first stage generated segmented objects and the second stage predicted the class of each object [62]. The method were applied to multispectral images to identify the regions of crops, weeds and soil with a mean accuracy 92.0% and an mAP 97.4%. Another study adopted a conventional algorithm using HSV-colour room vegetation index method for segmentation and a CNN for classification [65]. It achieved an F-score 98.6 and a mean accuracy 97.9% on an in-house RGB image dataset containing carrots, weeds and soil.

FCNs were investigated in pursuit of end-to-end solutions which treat the segmentation and classification within one neural network. In [68, 69], the last FC layer of a VGG-16 was replaced as a deconvolutional layer. The modified VGG-16 was evaluated on two RGB datasets: one to segment maize, weeds and soil and an mIoU 84.0% and a mean accuracy 95.4% was achieved; on another to segment equipment, soil, stump, weeds, grass, radish and unknown categories, a mean accuracy 79.0% was achieved. A FCN with a DenseNet backbone [63] was evaluated to identify crops, weeds and soil in multispectral images and achieved F-Scores 86.6% and 92.4% on two datasets collected from sugar beet fields in two different locations. Two FCN-8s were trained to segment RGB images: the first one recognized grass, clover, weeds and soil, and the latter one recognized fine-grained clover species including white clover and red clover [41]. It achieved

an mIoU 55.0 on its proposed GrassClover dataset.

In addition to using simple FCNs, recent studies tended to explore FCNs with additional mechanisms that are beneficial for segmentation tasks. In [38], a SegNet with VGG-16 backbone achieved a mean accuracy 64.1% on a carrot-weed dataset containing RGB images of carrots, weeds and soil. In [44], a public multispectral dataset - Sugar beet/Weed - was proposed to identify crops, weeds and soil, and a SegNet with a VGG-16 backbone achieved an F-Score 80.0 and an AUC 78.0 by evaluating the crops and the weeds predictions within a binary pixel-wise classification scheme. In [70], a SegNet with a ResNet-50 backbone was adopted to identify canola and weeds in RGB images using a pre-processing step to remove backgrounds, which achieved an mIoU 82.9 and a mean accuracy 99.5%. A Bonnet framework [73] to segment sunflower, weed and soil in RGB images achieved an mIoU 0.8 [66]. A customized U-Net with different data augmentation strategies was investigated for the CWFID dataset [36], which achieved an F-score 83.4. A VGG-UNet was evaluated for the Sugar beet/Weed dataset and achieved a mean accuracy 95.0% [64]. DeepLab-v3 was evaluated on Sugarbeet2016 containing multispectral and depth data and an in-house RGB oilseed dataset, which achieved mIoU values of 87.1 and 88.9, respectively [37].

Lightweight models aiming for efficient segmentation were explored. In [67], light models were mixed together with the guidance of a large and accurate model Inception-V3. On the CWFID dataset, compared to the Inception-V3 with an accuracy 93.9% and 0.12 fps during the inference, 4 mixed lightweight models achieved an accuracy 90.3% with 1.83 fps. A customized CNN using a ResNet-10 backbone [39] with side outputs and short connections for multi-scale feature fusion achieved an F-score 98.0 and an mIoU 95.9 on the CWF-788.

#### *3.4.4. Weed Instance Segmentation*

There have been a few attempts at deploying instance segmentation algorithms for weed identification. A recent study adopted Mask R-CNN for field RGB images of two crop species and four weed species [74]. Further explorations for this approach are needed by considering the perspectives such as the

improvements on different growth stage and small size plants.

## 4. Discussions

In this section, based on the current weed management studies and the recent developments of deep learning techniques, we discuss the challenges and opportunities for further advancing weed identification research from the following aspects: fine-grained learning, real-time inference, explainability, weakly-supervised / unsupervised learning, and incremental learning.

### 4.1. Fine-grained Learning

As reviewed in Section 3.4, most of the existing weed identification methods were based on general deep architectures ignoring the challenge caused by the strong similarities of crops and weed species. Recently, 3 major categories of fine-grained deep methods were explored to address this challenge.

**Patch-based methods** based on the fact that the fine-grained details often occur at a local-level. With the patterns collected from each region, fused or aggregated methods can be used to compute the final outputs. For example, regional CNN based features can be collected according to the key points of human poses for fine-grained action recognition [75].

**High-order pooling based methods** were introduced to address fine-grained tasks as well, which did not require explicit patch proposals (e.g. [76]). In particular, for a given convolutional feature map  $\mathbf{X} \in \mathbf{R}^{c \times wh}$ , the bilinear pooling can be computed by  $\mathbf{X}^\top \mathbf{X}$ ; the trilinear pooling can be computed by  $(\mathbf{X}^\top \mathbf{X})\mathbf{X}$ . The pooled vector can be used as the input of the subsequent layer of the network. The relations between the high-order pooling methods and the patch-based methods can be explained from the perspective of the attention [77]. Both of these methods result in focusing on the critical regions to collect efficient deep representations for their associated tasks.

**Regularization based methods** are based on that the intra-class difference could be higher than the inter-class difference for fine-grained modelling,

to introduce regularization terms for loss and drive the optimization to focus on learning fine-grained patterns. For example, in [78], pair-wise confusion and entropic confusion was introduced to construct its loss function.

Such fine-grained deep models provide a great opportunity to advance weed identification by taking the domain knowledge into account. For example, a weed can be decomposed into meaningful regions, such as leaves and stems. In our recent work, a patch-based GNN [54] was proposed towards fine-grained weed classification, which achieved an accuracy 98.1% on the DeepWeeds dataset, compared with the accuracy 95.3% of DenseNet.

#### *4.2. Real-time Inference*

While most of the weed identification studies demonstrated promising performance using deep learning techniques, these deep networks often contain a huge number of parameters. It leads to three major issues in regard to efficiency, memory consumption, and power consumption for deployment. Intuitively, as indicated in [79], lightweight models (e.g. MobileNet [80]) can be devised by using mechanisms such as parameter pruning, low-rank factorization, transferred/compact convolutional filters. In particular, using a Google Pixel 3 device with one-thread on a single large core, the inference time of MobileNet (V3) for image classification on ImageNet achieved a top-1 accuracy 65.4 and inference latency 11.7 ms. Note that these lightweight models can also be treated as backbones for object detection and segmentation. For example, SSDLite with MobileNet (V3) Small backbone achieved an inference latency of 43 ms and an mAP 16.1 on COCO test set; MobileNet (V3) based segmentation achieved an mIoU 69.4 with an inference time of 1.03s for an input image with resolution of  $1024 \times 2048$ . For weed identification, a ResNet-10 was proposed as backbone and introducing side outputs and short connections for multi-scale feature fusion. It achieved an mIoU 95.9 and an F-score 98.0, while the average inference latency is around 180ms on an Nvidia Jetson TX2 [39].

In addition to devising lightweight architectures, methods such as quantization and knowledge distillation are devised for any existing models with less



Table 4: Examples of real-time inference latency (ms) and performance for weed detection.

| Architecture                                | Modality      | Latency | Performance Metrics | Device          |
|---|---------------|---------|---------------------|-----------------|
| Customized CNN with ResNet-10 Backbone [39] | RGB           | 180     | 95.9 mIoU           | Jetson TX2      |
| Binarized DenseNet-128-32 [53]              | RGB           | 1.539   | 90.1 Acc            | Terasic DE1-SoC |
| Mixture of lightweight models [67]          | Multispectral | 546-934 | 90.0 Acc            | GeForce Titan X |

parameters while providing comparable performance as the complex models (e.g. ResNet-50 *vs.* ResNet-152). Quantization methods, which reduce the number of bits to represent the parameters in a model. In particular, binarization only saves one bit for parameter, which significantly reduces the memory consumption and computational cost [81]. A binarized DenseNet-128-32 was implemented by FPGA (Terasic DE1-SoC) for weed detection gaining an accuracy 88.91% [53]. It was slightly lower than a general DenseNet but obtained a very fast average inference latency 1.539ms. Knowledge distillation follows a similar way in which human beings learn, which contains one or more large pre-trained teacher models and a small student model. It aims to obtain an efficient student model which mimics and performs comparably to the teacher models. A distillation loss penalizes the difference between the outputs from the teacher and the student models. A weed identification study followed this scheme to obtain a few lightweight models for semantic segmentation [67]. Mixing these lightweight models achieved an accuracy 90.0% and the inference latency between 934ms to 546ms by using an Nvidia GeForce Titan X graphics card.

#### 4.3. Weakly-supervised & Unsupervised Learning

As manually collected supervision information for weed dataset can be resource expensive, weakly-supervised and unsupervised learning algorithms are needed for weed identification. For weakly-supervised learning, it is expected that weed object detection or even weed segmentation can be conducted when only using image-level annotation. For unsupervised learning, deep clustering and domain adaptation can be conducted. Deep clustering categorizes similar samples into one cluster in line with some similarity measures on their deep representations [82]. An application of deep clustering is that pre-training a

neural network with a large unlabelled dataset and further fine-tuning on a small labelled dataset. Domain adaptation solves the problem that the training samples and testing samples following different distributions. This could be the case, for example, two datasets for the same species are from different locations. Therefore, unsupervised domain adaptation handles situations where a network is trained on labeled data from a source domain and unlabeled data from a related but different target domain. Readers can refer to [83] for more details.

Note that existing deep learning based weed identification methods have not adequately explored this realm to use the unlabelled samples. Until very recently, deep clustering was investigated for weed image classification [72], in which a VGG-16 based DeepCluster network achieved an accuracy 70.6% on the DeepWeeds dataset. In [54], a GraphWeeNet involved a weakly-supervised learning strategy, namely multi-instance learning, and used image-level annotations to provide a rough locations of weed plants.

#### *4.4. Explainable Learning*

Deep learning shows a black-box nature, since it is difficult to understand and interpret the relations between the inputs and the outputs. However, explainability is of great importance for building trust between models and users to eventually facilitate the model adoption. As summarized in [84], there are three major approaches in pursuit of the explainability of deep learning: 1) visualization methods identify the most important parts of an input, which highly influence the results; 2) model distillation involves conventional machine learning models, most of which have clear statistical explanations and indications, to mimic the behavior of trained deep models; 3) intrinsic methods integrate mechanisms (e.g., the attention mechanisms).

Explainable learning has been seldom investigated for deep learning based weed identification, although it has the potentials to provide further insights. Recently, graph weeds net was proposed with its graph mechanism, which treats the regions of an input image as graph vertices, to analyze the critical regions [54]. As it usually takes more efforts for object detection or segmentation than

image classification, such explainable learning approach also provides an opportunity to take less effort to focus on the critical objects within an image. Furthermore, the critical regions are obtained without regional annotations, which can be viewed as a weakly-supervised learning requiring less human efforts.

#### 4.5. Incremental Learning

Most of the existing weed identification methods assume that a trained network will only deal with fixed target species, which are available during the training. As a result, when new species of interests are emerged, it is generally expected that the deep model needs to be re-trained with a new training set. To address this time-consuming and inflexible scheme, incremental learning is proposed to extends a trained model for new classes without the re-training from scratch. Note that the training samples of existing species are often not stored with a high volume due to storage limitations, whilst samples of incremental species could be adequate. Hence, incremental learning mainly addresses this imbalance nature when obtaining a new model based on an existing model.

To conduct incremental learning, 4 major approaches were investigated [85]. 1) retaining a subset of the old training data in line with a budget. 2) The distributions of the old dataset can be stored as the parameters of a generative model, which can produce unlimited samples during the incremental training. 3) Parameter isolation-based methods aim to prevent any possible forgetting of the previous tasks when no constraints on the model size. In general, for different species, it can use different model parameters to conduct the classification. 4) Regularization techniques prevent forgetting previous knowledge.

Recently, AgroAVNET explored the chance for incremental learning on the plant seedling dataset [52] and the accuracy achieved 91.35 for 12 species, compared to 93.64 from a general re-training. It followed a very straightforward way without fully exploiting the incremental learning, which froze the convolution layers trained by the original dataset and re-trained the FC layers only.

#### 4.6. Large Scale Dataset

Large scale datasets are essential for developing high performance and robust deep learning models. For example, ImageNet [13], which contains 15 million labeled images belonging to roughly 22,000 categories, has played a significant role in advancing deep learning based vision tasks. However, as summarized in Section 3.1, most of the existing weed datasets contain images of a small number of classes. In addition, those images were collected under limited scenarios, such as one growth stage and one light condition. This has limited the development of advanced methods applicable to a large variety of fields and prevents the translation towards commercial adoption. Therefore, constructing large scale datasets with diverse and complex conditions in the context of practical deployment can be highly demanded.

### 5. Conclusion

In this paper, we reviewed the recent progresses in the field of deep learning based weed identification and discussed the challenges and opportunities for future research. After introducing the fundamentals of deep learning techniques, we provided a systematical review from three aspects: research data, evaluation, and weed identification methods. There have been more than 10 public datasets collected through different modalities and many weed identification methods have been reported across different research disciplines due to the inter-disciplinary nature of this topic. It is also noticed that most existing weed identification methods were proposed by using the architectures developed for generic deep learning problems. Finally, we discussed the challenges and opportunities in terms of 5 different learning techniques and large scale dataset. Overall, deep learning based weed identification has gained increasing interest from different research communities and we feel that large scale datasets are strongly needed to bring this research direction to a new level.

## Acknowledgement

Funding: This work was supported by the GRDC (Grains Research and Development Corporation) [grant number 9177493].

## References

- [1] R. Llewellyn, D. Ronning, M. Clarke, A. Mayfield, S. Walker, and J. Ouzman, “Impact of weeds in Australian grain production,” *Grains Research and Development*, 2016.
- [2] Y. Gharde, P. Singh, R. Dubey, and P. Gupta, “Assessment of yield and economic losses in agriculture due to weeds in India,” *Crop Protection*, vol. 107, pp. 12–18, 2018.
- [3] G. R. Y. Coleman, A. Stead, M. P. Rigter, Z. Xu, D. Johnson, G. M. Brooker, S. Sukkariéh, and M. J. Walsh, “Using energy requirements to compare the suitability of alternative methods for broadcast and site-specific weed control,” *Weed Technology*, vol. 33, no. 4, pp. 633–650, 2019.
- [4] A. Olsen, D. A. Konovalov, B. Philippa, P. Ridd, J. C. Wood, J. Johns, W. Banks, B. Girgenti, O. Kenny, J. Whinney, *et al.*, “Deepweeds: A multiclass weed species image dataset for deep learning,” *Scientific Reports*, vol. 9, no. 1, p. 2058, 2019.
- [5] J. Charters, Z. Wang, Z. Chi, A. C. Tsoi, and D. D. Feng, “Eagle: a novel descriptor for identifying plant species using leaf lamina vascular features,” in *IEEE International Conference on Multimedia and Expo Workshops*, pp. 1–6, IEEE, 2014.
- [6] C. Cortes and V. Vapnik, “Support-vector networks,” *Machine Learning*, vol. 20, no. 3, pp. 273–297, 1995.
- [7] J. Schmidhuber, “Deep learning in neural networks: An overview,” *Neural Networks*, vol. 61, pp. 85–117, 2015.

- [8] J. Gu, Z. Wang, J. Kuen, L. Ma, A. Shahroudy, B. Shuai, T. Liu, X. Wang, G. Wang, J. Cai, *et al.*, “Recent advances in convolutional neural networks,” *Pattern Recognition*, vol. 77, pp. 354–377, 2018.
- [9] M. D. Zeiler, D. Krishnan, G. W. Taylor, and R. Fergus, “Deconvolutional networks,” in *IEEE Conference on Computer Vision and Pattern Recognition*, pp. 2528–2535, IEEE, 2010.
- [10] J. Bruna, W. Zaremba, A. Szlam, and Y. LeCun, “Spectral networks and locally connected networks on graphs,” *arXiv preprint arXiv:1312.6203*, 2013.
- [11] P. Veličković, G. Cucurull, A. Casanova, A. Romero, P. Liò, and Y. Bengio, “Graph attention networks,” in *International Conference on Learning Representations*, 2018.
- [12] V. K. Garg, S. Jegelka, and T. Jaakkola, “Generalization and representational limits of graph neural networks,” *arXiv preprint arXiv:2002.06157*, 2020.
- [13] A. Krizhevsky, I. Sutskever, and G. E. Hinton, “ImageNet classification with deep convolutional neural networks,” in *Advances in Neural Information Processing Systems*, pp. 1097–1105, 2012.
- [14] K. Simonyan and A. Zisserman, “Very deep convolutional networks for large-scale image recognition,” *arXiv preprint arXiv:1409.1556*, 2014.
- [15] C. Szegedy, S. Ioffe, V. Vanhoucke, and A. A. Alemi, “Inception-v4, inception-resnet and the impact of residual connections on learning,” in *AAAI Conference on Artificial Intelligence*, 2017.
- [16] G. Huang, Z. Liu, L. v. d. Maaten, and K. Q. Weinberger, “Densely connected convolutional networks,” in *IEEE Conference on Computer Vision and Pattern Recognition*, pp. 2261–2269, July 2017.

- [17] B. Zoph, V. Vasudevan, J. Shlens, and Q. V. Le, “Learning transferable architectures for scalable image recognition,” in *IEEE Conference on Computer Vision and Pattern Recognition*, pp. 8697–8710, 2018.
- [18] S. Ren, K. He, R. Girshick, and J. Sun, “Faster R-CNN: Towards real-time object detection with region proposal networks,” in *Advances in neural information processing systems*, pp. 91–99, 2015.
- [19] J. Redmon, S. Divvala, R. Girshick, and A. Farhadi, “You only look once: Unified, real-time object detection,” in *IEEE Conference on Computer Vision and Pattern Recognition*, pp. 779–788, 2016.
- [20] W. Liu, D. Anguelov, D. Erhan, C. Szegedy, S. Reed, C.-Y. Fu, and A. C. Berg, “Ssd: Single shot multibox detector,” in *European conference on computer vision*, pp. 21–37, Springer, 2016.
- [21] T.-Y. Lin, P. Goyal, R. Girshick, K. He, and P. Dollár, “Focal loss for dense object detection,” in *IEEE International Conference on Computer Vision*, pp. 2980–2988, 2017.
- [22] Z. Tian, C. Shen, H. Chen, and T. He, “Fcos: Fully convolutional one-stage object detection,” in *IEEE International Conference on Computer Vision*, pp. 9627–9636, 2019.
- [23] J. Long, E. Shelhamer, and T. Darrell, “Fully convolutional networks for semantic segmentation,” in *IEEE Conference on Computer Vision and Pattern Recognition*, pp. 3431–3440, 2015.
- [24] O. Ronneberger, P. Fischer, and T. Brox, “U-net: Convolutional networks for biomedical image segmentation,” in *International Conference on Medical Image Computing and Computer-assisted intervention*, pp. 234–241, Springer, 2015.
- [25] V. Badrinarayanan, A. Kendall, and R. Cipolla, “Segnet: A deep convolutional encoder-decoder architecture for image segmentation,” *IEEE*

*Transactions on Pattern Analysis and Machine Intelligence*, vol. 39, no. 12, pp. 2481–2495, 2017.

- [26] H. Zhao, J. Shi, X. Qi, X. Wang, and J. Jia, “Pyramid scene parsing network,” in *IEEE Conference on Computer Vision and Pattern Recognition*, pp. 2881–2890, 2017.
- [27] L.-C. Chen, Y. Zhu, G. Papandreou, F. Schroff, and H. Adam, “Encoder-decoder with atrous separable convolution for semantic image segmentation,” in *European Conference on Computer Vision*, pp. 801–818, 2018.
- [28] K. He, G. Gkioxari, P. Dollár, and R. Girshick, “Mask R-CNN,” in *IEEE International Conference on Computer Vision*, pp. 2961–2969, 2017.
- [29] G. Papandreou, T. Zhu, L.-C. Chen, S. Gidaris, J. Tompson, and K. Murphy, “Personlab: Person pose estimation and instance segmentation with a bottom-up, part-based, geometric embedding model,” in *European Conference on Computer Vision*, pp. 269–286, 2018.
- [30] D. Bolya, C. Zhou, F. Xiao, and Y. J. Lee, “Yolact: Real-time instance segmentation,” in *IEEE International Conference on Computer Vision*, pp. 9157–9166, 2019.
- [31] Y. Li, H. Qi, J. Dai, X. Ji, and Y. Wei, “Fully convolutional instance-aware semantic segmentation,” in *IEEE Conference on Computer Vision and Pattern Recognition*, pp. 2359–2367, 2017.
- [32] E. Xie, P. Sun, X. Song, W. Wang, X. Liu, D. Liang, C. Shen, and P. Luo, “Polarmask: Single shot instance segmentation with polar representation,” in *IEEE Conference on Computer Vision and Pattern Recognition*, pp. 12193–12202, 2020.
- [33] H. Chen, K. Sun, Z. Tian, C. Shen, Y. Huang, and Y. Yan, “Blendmask: Top-down meets bottom-up for instance segmentation,” in *IEEE Conference on Computer Vision and Pattern Recognition*, pp. 8573–8581, 2020.



- [34] J. Machleb, G. G. Peteinatos, B. L. Kollenda, D. Andújar, and R. Gerhards, “Sensor-based mechanical weed control: Present state and prospects,” *Computers and Electronics in Agriculture*, vol. 176, p. 105638, 2020.
- [35] A. Farooq, J. Hu, and X. Jia, “Analysis of spectral bands and spatial resolutions for weed classification via deep convolutional neural network,” *IEEE Geoscience and Remote Sensing Letters*, vol. 16, no. 2, pp. 183–187, 2018.
- [36] A. Brilhador, M. Gutoski, L. T. Hattori, A. de Souza Inácio, A. E. Lazaretti, and H. S. Lopes, “Classification of weeds and crops at the pixel-level using convolutional neural networks and data augmentation,” in *IEEE Latin American Conference on Computational Intelligence*, pp. 1–6, IEEE, 2019.
- [37] A. Wang, Y. Xu, X. Wei, and B. Cui, “Semantic segmentation of crop and weed using an encoder-decoder network and image enhancement method under uncontrolled outdoor illumination,” *IEEE Access*, vol. 8, pp. 81724–81734, 2020.
- [38] P. Lameski, E. Zdravevski, V. Trajkovik, and A. Kulakov, “Weed detection dataset with rgb images taken under variable light conditions,” in *International Conference on ICT Innovations*, pp. 112–119, Springer, 2017.
- [39] N. Li, X. Zhang, C. Zhang, H. Guo, Z. Sun, and X. Wu, “Real-time crop recognition in transplanted fields with prominent weed growth: a visual-attention-based approach,” *IEEE Access*, vol. 7, pp. 185310–185321, 2019.
- [40] S. Haug and J. Ostermann, “A crop/weed field image dataset for the evaluation of computer vision based precision agriculture tasks,” in *European Conference on Computer Vision*, pp. 105–116, Springer, 2014.
- [41] S. Skovsen, M. Dyrmann, A. K. Mortensen, M. S. Laursen, R. Gislum, J. Eriksen, S. Farkhani, H. Karstoft, and R. N. Jorgensen, “The grassclover

- image dataset for semantic and hierarchical species understanding in agriculture,” in *IEEE Conference on Computer Vision and Pattern Recognition Workshops*, pp. 0–0, 2019.
- [42] T. M. Giselsson, R. N. Jørgensen, P. K. Jensen, M. Dyrmann, and H. S. Midtiby, “A public image database for benchmark of plant seedling classification algorithms,” *arXiv preprint arXiv:1711.05458*, 2017.
- [43] N. Chebrolu, P. Lottes, A. Schaefer, W. Winterhalter, W. Burgard, and C. Stachniss, “Agricultural robot dataset for plant classification, localization and mapping on sugar beet fields,” *The International Journal of Robotics Research*, vol. 36, no. 10, pp. 1045–1052, 2017.
- [44] I. Sa, Z. Chen, M. Popović, R. Khanna, F. Liebisch, J. Nieto, and R. Siegwart, “weednet: Dense semantic weed classification using multispectral images and mav for smart farming,” *IEEE Robotics and Automation Letters*, vol. 3, no. 1, pp. 588–595, 2017.
- [45] H. Jiang, C. Zhang, Y. Qiao, Z. Zhang, W. Zhang, and C. Song, “CNN feature based graph convolutional network for weed and crop recognition in smart farming,” *Computers and Electronics in Agriculture*, vol. 174, p. 105450, 2020.
- [46] V. Nguyen Thanh Le, B. Apopei, and K. Alameh, “Effective plant discrimination based on the combination of local binary pattern operators and multiclass support vector machine methods,” *Information Processing in Agriculture*, vol. 6, no. 1, pp. 116–131, 2019.
- [47] M. Dyrmann, H. Karstoft, and H. S. Midtiby, “Plant species classification using deep convolutional neural network,” *Biosystems Engineering*, vol. 151, pp. 72–80, 2016.
- [48] A. dos Santos Ferreira, D. M. Freitas, G. G. da Silva, H. Pistori, and M. T. Folhes, “Weed detection in soybean crops using convnets,” *Computers and Electronics in Agriculture*, vol. 143, pp. 314–324, 2017.

- [49] C. Shorten and T. M. Khoshgoftaar, “A survey on image data augmentation for deep learning,” *Journal of Big Data*, vol. 6, no. 1, p. 60, 2019.
- [50] A. Farooq, X. Jia, J. Hu, and J. Zhou, “Multi-resolution weed classification via convolutional neural network and superpixel based local binary pattern using remote sensing images,” *Remote Sensing*, vol. 11, no. 14, p. 1692, 2019.
- [51] M. D. Bah, A. Hafiane, and R. Canals, “Deep learning with unsupervised data labeling for weed detection in line crops in uav images,” *Remote sensing*, vol. 10, no. 11, p. 1690, 2018.
- [52] T. R. Chavan and A. V. Nandedkar, “Agroavnet for crops and weeds classification: A step forward in automatic farming,” *Computers and Electronics in Agriculture*, vol. 154, pp. 361–372, 2018.
- [53] C. Lammie, A. Olsen, T. Carrick, and M. R. Azghadi, “Low-power and high-speed deep fpga inference engines for weed classification at the edge,” *IEEE Access*, vol. 7, pp. 51171–51184, 2019.
- [54] K. Hu, G. Coleman, S. Zeng, Z. Wang, and M. Walsh, “Graph weeds net: A graph-based deep learning method for weed recognition,” *Computers and Electronics in Agriculture*, vol. 174, p. 105520, 2020.
- [55] J. Tang, D. Wang, Z. Zhang, L. He, J. Xin, and Y. Xu, “Weed identification based on k-means feature learning combined with convolutional neural network,” *Computers and Electronics in Agriculture*, vol. 135, pp. 63–70, 2017.
- [56] J. Yu, A. W. Schumann, Z. Cao, S. M. Sharpe, and N. S. Boyd, “Weed detection in perennial ryegrass with deep learning convolutional neural network,” *Frontiers in Plant Science*, vol. 10, 2019.
- [57] J. Yu, S. M. Sharpe, A. W. Schumann, and N. S. Boyd, “Deep learning for image-based weed detection in turfgrass,” *European Journal of Agronomy*, vol. 104, pp. 78–84, 2019.

- [58] W. Xinshao and C. Cheng, “Weed seeds classification based on pcanet deep learning baseline,” in *Asia-Pacific Signal and Information Processing Association Annual Summit and Conference*, pp. 408–415, IEEE, 2015.
- [59] A. N. V. Veeranampalayam Sivakumar, J. Li, S. Scott, E. Psota, A. J. Jhala, J. D. Luck, and Y. Shi, “Comparison of object detection and patch-based classification deep learning models on mid-to late-season weed detection in uav imagery,” *Remote Sensing*, vol. 12, no. 13, p. 2136, 2020.
- [60] M. Dyrmann, R. N. Jørgensen, and H. S. Midtiby, “Roboweedsupport-detection of weed locations in leaf occluded cereal crops using a fully convolutional neural network,” *Advances in Animal Bioscience*, vol. 8, no. 2, pp. 842–847, 2017.
- [61] S. M. Sharpe, A. W. Schumann, J. Yu, and N. S. Boyd, “Vegetation detection and discrimination within vegetable plasticulture row-middles using a convolutional neural network,” *Precision Agriculture*, vol. 21, no. 2, pp. 264–277, 2020.
- [62] C. Potena, D. Nardi, and A. Pretto, “Fast and accurate crop and weed identification with summarized train sets for precision agriculture,” in *International Conference on Intelligent Autonomous Systems*, pp. 105–121, Springer, 2016.
- [63] P. Lottes, J. Behley, A. Milioto, and C. Stachniss, “Fully convolutional networks with sequential information for robust crop and weed detection in precision farming,” *IEEE Robotics and Automation Letters*, vol. 3, no. 4, pp. 2870–2877, 2018.
- [64] M. Fawakherji, C. Potena, D. D. Bloisi, M. Imperoli, A. Pretto, and D. Nardi, “Uav image based crop and weed distribution estimation on embedded gpu boards,” in *International Conference on Computer Analysis of Images and Patterns*, pp. 100–108, Springer, 2019.

- [65] F. J. Knoll, V. Czymmek, S. Poczhoski, T. Holtorf, and S. Hussmann, “Improving efficiency of organic farming by using a deep learning classification approach,” *Computers and Electronics in Agriculture*, vol. 153, pp. 347–356, 2018.
- [66] M. Fawakherji, A. Youssef, D. Bloisi, A. Pretto, and D. Nardi, “Crop and weeds classification for precision agriculture using context-independent pixel-wise segmentation,” in *IEEE International Conference on Robotic Computing*, pp. 146–152, IEEE, 2019.
- [67] C. McCool, T. Perez, and B. Upcroft, “Mixtures of lightweight deep convolutional neural networks: Applied to agricultural robotics,” *IEEE Robotics and Automation Letters*, vol. 2, no. 3, pp. 1344–1351, 2017.
- [68] M. Dyrmann, A. K. Mortensen, H. S. Midtiby, R. N. Jørgensen, *et al.*, “Pixel-wise classification of weeds and crops in images by using a fully convolutional neural network,” in *International Conference on Agricultural Engineering*, pp. 26–29, 2016.
- [69] A. K. Mortensen, M. Dyrmann, H. Karstoft, R. N. Jørgensen, R. Gislum, *et al.*, “Semantic segmentation of mixed crops using deep convolutional neural network,” in *International Conference of Agricultural Engineering*, 2016.
- [70] M. H. Asad and A. Bais, “Weed detection in canola fields using maximum likelihood classification and deep convolutional neural network,” *Information Processing in Agriculture*, 2019.
- [71] D. C. Ciresan, U. Meier, L. M. Gambardella, and J. Schmidhuber, “Convolutional neural network committees for handwritten character classification,” in *International Conference on Document Analysis and Recognition*, pp. 1135–1139, IEEE, 2011.
- [72] A. dos Santos Ferreira, D. M. Freitas, G. G. da Silva, H. Pistori, and M. T. Folhes, “Unsupervised deep learning and semi-automatic data labeling in

- weed discrimination,” *Computers and Electronics in Agriculture*, vol. 165, p. 104963, 2019.
- [73] A. Milioto and C. Stachniss, “Bonnet: An open-source training and deployment framework for semantic segmentation in robotics using CNNs,” in *International Conference on Robotics and Automation*, pp. 7094–7100, IEEE, 2019.
- [74] J. Champ, A. Mora-Fallas, H. Goëau, E. Mata-Montero, P. Bonnet, and A. Joly, “Instance segmentation for the fine detection of crop and weed plants by precision agricultural robots,” *Applications in Plant Sciences*, vol. 8, no. 7, p. e11373, 2020.
- [75] K. Hu, Z. Wang, S. Mei, K. A. Ehgoetz Martens, T. Yao, S. J. G. Lewis, and D. D. Feng, “Vision-based freezing of gait detection with anatomic directed graph representation,” *IEEE Journal of Biomedical and Health Informatics*, vol. 24, no. 4, pp. 1215–1225, 2019.
- [76] H. Zheng, J. Fu, Z.-J. Zha, and J. Luo, “Looking for the devil in the details: Learning trilinear attention sampling network for fine-grained image recognition,” in *IEEE Conference on Computer Vision and Pattern Recognition*, pp. 5012–5021, 2019.
- [77] J.-H. Kim, J. Jun, and B.-T. Zhang, “Bilinear attention networks,” in *Advances in Neural Information Processing Systems*, pp. 1564–1574, 2018.
- [78] A. Dubey, O. Gupta, P. Guo, R. Raskar, R. Farrell, and N. Naik, “Training with confusion for fine-grained visual classification,” *CoRR*, vol. abs/1705.08016, 2017.
- [79] Y. Cheng, D. Wang, P. Zhou, and T. Zhang, “A survey of model compression and acceleration for deep neural networks,” *arXiv preprint arXiv:1710.09282*, 2017.

- [80] A. Howard, M. Sandler, G. Chu, L.-C. Chen, B. Chen, M. Tan, W. Wang, Y. Zhu, R. Pang, V. Vasudevan, *et al.*, “Searching for mobilenetv3,” in *IEEE International Conference on Computer Vision*, pp. 1314–1324, 2019.
- [81] H. Qin, R. Gong, X. Liu, X. Bai, J. Song, and N. Sebe, “Binary neural networks: A survey,” *Pattern Recognition*, p. 107281, 2020.
- [82] E. Min, X. Guo, Q. Liu, G. Zhang, J. Cui, and J. Long, “A survey of clustering with deep learning: From the perspective of network architecture,” *IEEE Access*, vol. 6, pp. 39501–39514, 2018.
- [83] G. Wilson and D. J. Cook, “A survey of unsupervised deep domain adaptation,” *ACM Transactions on Intelligent Systems and Technology*, vol. 11, no. 5, pp. 1–46, 2020.
- [84] N. Xie, G. Ras, M. van Gerven, and D. Doran, “Explainable deep learning: A field guide for the uninitiated,” *arXiv preprint arXiv:2004.14545*, 2020.
- [85] M. De Lange, R. Aljundi, M. Masana, S. Parisot, X. Jia, A. Leonardis, G. Slabaugh, and T. Tuytelaars, “Continual learning: A comparative study on how to defy forgetting in classification tasks,” *arXiv preprint arXiv:1909.08383*, 2019.